

Detection of bacterial wilt infection caused by *Ralstonia solanacearum* in potato (*Solanum tuberosum* L.) through multifractal analysis applied to remotely sensed data

Perla Chávez · Christian Yarlequé · Hildo Loayza · Víctor Mares ·
Paola Hanco · Sylvie Priou · María del Pilar Márquez ·
Adolfo Posadas · Percy Zorogastúa · Jaime Flexas · Roberto Quiroz

Published online: 19 August 2011
© Springer Science+Business Media, LLC 2011

Abstract Potato bacterial wilt, caused by the bacterium *Ralstonia solanacearum* race 3 biovar 2 (R3bv2), affects potato production in several regions in the world. The disease becomes visually detectable when extensive damage to the crop has already occurred. Two greenhouse experiments were conducted to test the capability of a remote sensing diagnostic method supported by multispectral and multifractal analyses of the light reflectance signal, to detect physiological and morphological changes in plants caused by the infection. The analysis was carried out using the Wavelet Transform Modulus Maxima (WTMM) combined with the Multifractal (MF) analysis to assess the variability of high-resolution temporal and spatial signals and the conservative properties of the processes across temporal and spatial scales. The multispectral signal, enhanced by multifractal analysis, detected both symptomatic and latently infected plants, matching the results of ELISA laboratory assessment in 100 and 82%, respectively. Although the multispectral method provided no earlier detection than the visual assessment on symptomatic plants, the former was able to detect asymptomatic latent infection, showing a great potential as a monitoring tool for the control of bacterial wilt in potato crops. Applied to precision agriculture, this capability of the remote sensing diagnostic methodology would provide a more efficient control of the disease through an early and full spatial assessment of the health status of the crop and the prevention of spreading the disease.

Keywords Remote sensing diagnostic method · Visual monitoring · Multispectral analysis · Wavelet transform · Precision agriculture

P. Chávez · C. Yarlequé · H. Loayza · V. Mares · P. Hanco · S. Priou ·
M. P. Márquez · A. Posadas · P. Zorogastúa · R. Quiroz (✉)
Crop Management and Production Systems Division, International Potato Center, Av. La Molina 1895,
Lima 12, Peru
e-mail: cip-pse@cgiar.org; r.quiroz@cgiar.org
URL: www.cipotato.org; www.uib.es

P. Chávez · J. Flexas
Research Group in Biology of Plants Under Mediterranean Conditions, University of Balearic Islands,
Crtra. Valldemossa km.7.5, 07122 Palma de Mallorca, Spain

Introduction

Bacterial wilt ranks among the most destructive potato diseases in Africa, Asia, and Central and South America (CABI 2003), causing yield losses of up to 75% (Cook and Sequeira 1994). It is caused by *Ralstonia solanacearum* Smith, a soil borne bacterium that typically invades plants through the roots and colonizes the xylem vessels. In an infected plant, vascular bundles are filled with multiplying bacteria that obstruct the transportation of water and nutrients, thus, symptoms include leaf yellowing, vascular browning and necrosis and wilting of the plant. Physiological changes, such as the increase of respiration rate and reduction of transpiration and photosynthesis, occur in infected plants (Chiwaki et al. 2005), which sometimes show a temporary recovery from wilting while the disease is progressing, or may not show any visible change before a sudden wilting. In any case, all diseased plants are seriously blighted in the end. Secondary infection occurs as the bacteria survive for a long time in the soil in the residues of diseased plants (Chiwaki et al. 2005).

Ralstonia solanacearum is classified into 5 races on the basis of host range, and 5 biovars on the basis of the ability of strains to oxidize three sugar alcohols and three disaccharides (Hayward 1964, 1991; Schaad 1988). The phylogenetically and phenotypically homogenous cluster known as race 3 biovar 2 (R3bv2) [Division II (Cook et al. 1989) and Phylotype II (Prior and Fegan 2005)] is the dominant race in the Andean region in South America where the potato and possibly this race of *R. solanacearum* originated. However, it is also present in mountain regions in other tropical areas as well as in the Mediterranean basin. The pathogen commonly causes latent (asymptomatic) infections in the cool tropical highlands, but when infected seed tubers are planted in warmer lowland fields, the resulting plants quickly wilt and die (Allen et al. 2001). R3bv2 was introduced into northern Europe around 1972 causing significant losses due both to disease incidence and to quarantine restrictions that require the destruction of infected crops and fallowing of infested fields (Elphinstone 1996; Janse 1996). The bacteria were probably disseminated by infected tubers and contaminated irrigation water (Williamson et al. 2002). Despite ongoing eradication efforts, *R. solanacearum* is still present in a large number of fields and waterways of northern Europe, although it has caused only minor direct crop losses (Elphinstone 1996). Recent ecological studies found that an R3bv2 strain could survive at least 12 months in temperate region soils and for at least 110 days in surface water at 12°C (van Elsas et al. 2000, 2001). *Solanum dulcamara*, a common semi-aquatic weed, is an important host and source of inoculum in Europe (Elphinstone 1996). R3bv2 is not known to be established in North America (Williamson et al. 2002; Swanson et al. 2005).

Many trials have been carried out all over the world to control the disease without much success. No significant control has been achieved by using antibiotics (Habashy et al. 1993), soil fumigants (Weingartner and Shumaker 1988), chemical control (Murakoshi and Takahashi 1984) or breeding of resistant varieties (Hartman and Elphinstone 1994; Mendoza 1994; Fock et al. 2001; López and Biosca 2004). Moreover, chemical control is nowadays a less desirable option due to the increasing demand for low-input and organically produced products to prevent the potential negative health effects of pesticides and chemical residues (Sylvander and Le Floc'h-Wadel 2000; Parrott and Kalibwani 2004).

Due to unsuccessful efforts to control the incidence of *R. solanacearum* around the world, early detection of the disease is highly necessary as the source of secondary infection is significantly reduced by the early removal of diseased plants (Chiwaki et al. 2005). Thermal infrared imagery showed that stress-induced reduction of photosynthesis, transpiration and stomatal conductance are closely related to an increase in leaf temperature in plants (Inoue 1990; Chiwaki et al. 2005). Using this method, Chiwaki et al. (2005)

were able to determine bacterial infection in plants 4 days earlier than the visual identification of symptoms, as the invasion of vascular bundles by multiplying bacteria reduced transpiration and caused a raised leaf temperature. Another promising technique is remote sensing and spectroradiometry of plant reflectance as it allows the early detection of morphological and anatomical changes even if these changes are small, as shown for virus infection (Chávez et al. 2009, 2010). Our own unpublished work provides evidence that the technique is also able to detect changes caused by water stress in plants. The reflectance pattern of healthy and stressed (infected) potato plants—in the visible and NIR range of the spectrum—are expected to differ due to different physiological and ontogenetical responses of the two groups of plants. Changes in the reflectance, as the normal plant ages, are related to changes in the ratio of new to aged leaves, which have different concentrations of pigments that absorb light in the visible range of the spectrum (UA 2005). With the onset of translocation of assimilates from the foliage to the tubers, the leaves initiate a rapid senescence process (Buchanan-Wollaston 1997) that spectrally resembles the effect produced by stressors in a stressed plant. However, the effects of biotic or abiotic stressors disrupt the normal timing and pattern change of reflectance that occurs in a healthy plant along its development from emergence to maturity. This departure from a normal reflectance pattern along time, difficult to be visually noticed at early stages, calls for the development of a reliable method for the early detection of stress responses to agents such as bacteria, viruses, and drought periods, based on non-conventional data processing techniques (Chávez et al. 2010). In this work, the wavelet-based multifractal approach was used.

Based on preliminary results that showed the sensitivity of reflectance patterns to mirror changes in metabolism of potato plants, we hypothesized that wavelet-based multifractal analysis of time series of multispectral reflectance of plants could be used for diagnosing bacterial wilt infection. We assumed that signals not readily evident in the time domain could be seen in the frequency domain. Indeed, the diagnostic capability of time-series reflectance signals has been shown to be enhanced by the wavelet-based multifractal analysis as the wavelet transform is capable of providing time and frequency information simultaneously, hence giving a time–frequency representation of the signal. Multifractal techniques are increasingly recognized as the most appropriate and straightforward framework for analyzing and simulating not only the scale dependency of geophysical observables, but also their extreme variability over a wide range of scales (Schertzer and Lovejoy 2004). Multifractal theory permits the characterization of complex phenomena in a fully quantitative fashion, for continuous signals (e.g. time, space or wavelength) (Vicsek 1992). An important property of multifractal systems is that they are scale invariant (Schertzer and Lovejoy 1989), which means that the information they provide is constant across different scales, allowing for a valid extrapolation up and down scales. This property of the multifractal analysis is particularly relevant in the work herewith reported, as it was hypothesized that it would confer robustness and consistency to the analysis of observed data. Moreover, the multifractal analysis gives a description of several physical properties of the observed signal such as the internal entropy, the anisotropy and the correlation among data. Indeed, multifractal analysis has been applied to signal data in several research fields such as solar flare X-ray emissions (McAteer et al. 2007) soil science (Posadas et al. 2003, 2005), neurology (Yu et al. 2001; Latka et al. 2002) and cardiology (Ivanov et al. 1999; Byalovskii et al. 2005) among others. Hence, the objective of this work was to test the feasibility of using the multispectral light reflectance of plants, supported by conventional and wavelet-based multifractal analyses of the reflectance signal, for detecting *R. solanacearum* infection in potato crops, aiming at developing a

practical field monitoring method for the spatial assessment of the health condition of the crop. Although this work is methodologically similar to that reported in Chávez et al. (2009, 2010), it is different in the sense that it tries to look for a general application of the diagnostic tool to different stresses which generally cause different physiological and morphological changes in affected plants. The general hypothesis is that different plant reactions, caused by a diversity of stressors (e.g. virus, bacteria, water deficits, heat and cold) could be detected by the tested sensing devices and analytical methods.

Materials and methods

Plant material

Two greenhouse experiments were conducted under a split-plot in time design in Lima, Peru, during the autumn and winter, 2007. Two potato cultivars with different resistance to *R. solanacearum* were tested: 30 plants of Canchán, a non-resistant cultivar, were used in the first experiment and 30 plants of Costanera, a resistant cultivar, were used in the second one. In both experiments, germinated tubers were planted into a 30 × 45 cm plastic tray containing Promix Bx substrate. After 2 weeks, 15 rooted plants in each experiment were transplanted into individual plastic pots containing 800 g of substrate (mush, sand and soil in a proportion of 3:1:1) previously inoculated with *R. solanacearum*. Also, in each experiment 15 plants transplanted into non-inoculated substrate were used as negative controls.

Bacterial inoculation

Ralstonia solanacearum was grown in a modified Kelman's medium (MKM) (French et al. 1995) without tetrazolium chloride (TZC) and then incubated at 30°C for 48 h. Approximately 10 ml of sterile distilled water were added to each plate and bacterial colonies were stirred using a sterile cotton swab. The resulting bacterial suspension was standardized using a spectrophotometer Spectronic 20 (Bausch & Lomb, USA) under a 600 nm wavelength light until obtaining an optic density of 0.1 absorbance, which is equivalent to a concentration of approximately 2×10^8 CFU ml⁻¹. One day before transplanting the plants, the inoculum was added to the substrate up to a concentration of 10^6 cells g⁻¹ of substrate.

Reflectance data acquisition

Solar radiation reflected by individual plants was periodically recorded before and after transplanting using a computer assisted Li-Cor Li-1800 spectroradiometer (Li-Cor Inc., Lincoln, Nebraska, USA) covering the 350–850 nm wavelength region with a spectral resolution of 4 nm. As the Li-1800 spectroradiometer has a built-in cosine corrector, the aperture angle of the fore optics of the spectroradiometer was 60° and measurements were performed from nadir. Before measurements were taken, a white barium sulfate panel was placed under the fore optics at the same distance of the plant canopy and the reflected radiance was used for the calibration of the equipment. Incident radiation flux on the canopy was measured by facing the sensor to the Sun and the reflected flux was calculated by the immediate measurement of light intensity registered by the faced-down sensor

located some 0.20 m over the canopy, resulting in a circular field of view of 20 cm diameter. Three daily reflectance measurements per plant were taken using the white panel and the relative reflectance values were averaged to estimate its spectral variability. Measurements were carried out during approximately 25 days, from one or 2 days before the bacteria inoculation of substrate, and then after transplanting until the appearance of symptoms in the plants.

Visual evaluation of infection symptoms

Visual assessments (mainly based on chlorosis and wilting of leaves) of both control and exposed plants were carried out every 2 days to monitor the development of disease symptoms. At the end of each experiment, plants were individually tested for the presence of the bacteria using the CIP post enrichment NCM-ELISA kit (Priou et al. 1999), which per se does not discriminate latent from active infection, but only confirm or discard the presence of the bacteria in the analyzed tissue. Therefore, active infection is defined by the concurrence of disease symptoms and bacteria in the plant, while a latent infection occurs when an infected plant appears healthy (symptomless) at visual inspection.

Data analysis

Quantification of discrete reflectance by bands

A method previously used for virus (PYVV) detection in potato (Chávez et al. 2009, 2010) was slightly modified by splitting the reflection spectra into 4 discrete bands to mimic those of the Landsat TM: blue (450–520 nm), green (520–600 nm), red (630–690 nm) and NIR (760–900 nm). The proportion of the reflected radiation per band relative to the total of the four bands was calculated as a function of time (growth), resulting in a heterogeneous reflectance spectra displaying anomalies through time. This assessment was carried out with data from the two experiments to contrast the obtained information with the results of the wavelet-multifractal analysis of the continuous spectra. Also, several spectral vegetation indices (Table 1) were calculated to assess their accuracy in detecting the health condition of the crop as affected by the bacterial wilt disease.

Wavelet based multifractal data analysis

The Multifractal Formalism relies on the fact that the highly non-uniform probability distributions arising from the non-uniformity of the system often possess rich scaling properties, as shown in Fig. 1. In a multifractal signal system, the behavior around any point can be described by the Hölder exponents ($h(x)$) that quantify the local regularity of a signal around the point x and is called the *singularity exponent*. The ensemble formed by all the points that share the same singularity exponent is a fractal set of fractal dimension ($D(h)$). The curve of $D(h)$ against h is called the *multifractal spectrum* that fully describes the statistical distribution of the system. Thus, $D(h)$ relates each group of data having the same singularity (represented by h). It has been demonstrated (Chhabra et al. 1989a, b) that $D(h)$ corresponds to the entropy density of the system, while the set of h is related with its internal energy, according to thermodynamic principles. Muzy et al. (1991), Arneodo et al. (1995) and Bacry et al. (2003) developed a statistical method for the estimation of the *multifractal spectrum* based on the study of the maxima of the continuous wavelet

Table 1 Spectral Vegetation Indexes (SVIs) calculated from multispectral reflectance of potato plants

SVI	Aim	Equation	References
Normalized Difference Vegetation Index (NDVI)	Structural	$(R_{NIR} - R_{red}) / (R_{NIR} + R_{red})$	Rouse et al. (1974)
Soil Adjusted Vegetation Index (SAVI)	Structural	$[(R_{NIR} - R_{red}) / (R_{NIR} + R_{red} + L)] * (1 + L)$	Huete (1988)
Infrared Percentage Vegetation Index (IPVI)	Structural	$R_{red} / (R_{NIR} + R_{red})$	Crippen (1990)
Photochemical Reflectance Index (PRI)	Physiological	$(R_{570} - R_{531}) / (R_{570} + R_{531})$	Gamon et al. (1992)
Modified Chlorophyll Absorption Index (MCARI)	Chlorophyll	$[(R_{700} - R_{670}) - 0.2 (R_{700} - R_{550})] * (R_{700} / R_{670})$	Daughtry et al. (2000)
Transformed Chlorophyll Absorption Index	Chlorophyll	$3 * [(R_{700} - R_{670}) - 0.2 * (R_{700} - R_{550}) * (R_{700} / R_{670})]$	Haboudane et al. (2002)
Optimized Soil-Adjusted Vegetation Index	Structural	$(1 + 0.16) * (R_{800} - R_{670}) / (R_{800} + R_{670} + 0.16)$	Rondeaux et al. (1996)
Triangular Vegetation Index	Chlorophyll	$0.5 * [120 * (R_{750} - R_{550}) - 200 * (R_{670} - R_{550})]$	Broge and Leblanc (2000)
Modified Triangular Vegetation Index 1	Structural	$1.2 * [1.2 * (R_{800} - R_{550}) - 2.5 * (R_{670} - R_{550})]$	Haboudane et al. (2004)

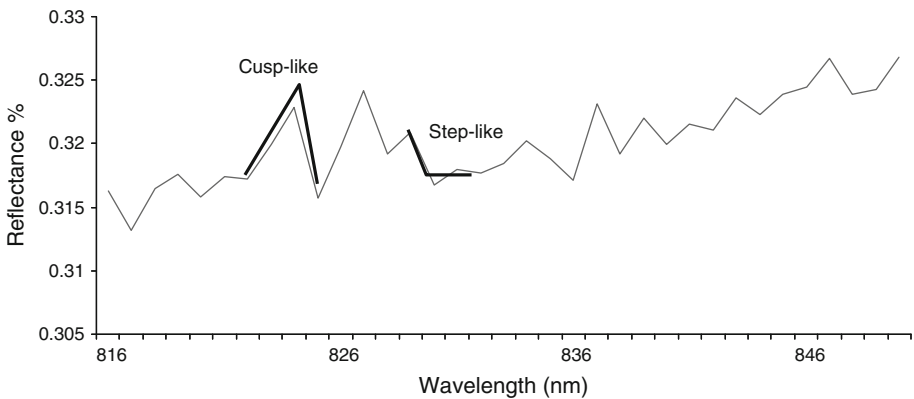


Fig. 1 Heterogeneous signal of a reflectance spectrum showing two types of singularities: step-like and cusp-like features

transform of the signal. This method is known as the Wavelet Transform Modulus Maxima Method (WTMM), which we used for the reflectance signal analysis to obtain the *multi-fractal spectrum*. As light has properties of both waves and particles, the wavelet based multifractal analysis is suitable to be applied to light reflectance data.

McAteer et al. (2007) showed the equations for obtaining the multifractal parameters h and $D(h)$, through their *scale invariance property*. This means that the statistical physics property is conserved across scales (from fine to coarse), thus providing a more accurate characterization of the phenomenon under study. These parameters depend on the order statistical moments “ q ”. For example, $q = 1$ gives the first statistical moment or mean, $q = 2$ gives the second statistical moment and its association with the variance value, and

so on. In Multifractal theory the analysis is conducted along a defined q range, yielding the description of its statistical behavior. In a practical way, the existence of scale invariance property is portrayed by the linear behavior in the partition function $D(h(q))$ against $\log[\text{scale}]$, and partition function $h(q)$ against $\log[\text{scale}]$ graphs by each q -values where the slopes correspond to $D(h)$ and h , respectively, as described by McAteer et al. (2007)

The continuous wavelet transform of the $S(\lambda)$ signal (λ is the wavelength variable) is defined as follows:

$$CWT_S^\psi(b, a) = \frac{1}{\sqrt{|a|}} \int S(\lambda) \psi * \left(\frac{\lambda - b}{a} \right) d\lambda, \quad (1)$$

Equation 1 shows that the transformed signal of $S(\lambda)$, is a function of two variables, b and a , the translation and scale parameters, respectively. ψ is the transforming function, and is called the *mother wavelet*, being ψ^* its complex conjugate (Polikar 1996). The term *mother wavelet* owes its name to two important properties of the wavelet analysis: First, the term *wavelet* refers to a small wave. The condition of being small is related to the fact that this (window) function is of finite length (compactly supported). The *wave* condition indicates that this function is oscillatory. The term *mother* implies that the functions with different regions of support used in the transformation process are derived from one main function, or the mother wavelet. In other words, the mother wavelet is a prototype for generating the other window functions. Secondly, the term *translation* is related to the location of the window, as the window is shifted through the signal and corresponds to time information in the transform domain. However, we do not have directly a frequency parameter. Instead, we have a *scale* parameter which is inversely proportional to frequency. The parameter *scale* in the wavelet analysis is similar to the scale used in maps. As in the case of maps, high scales correspond to a non-detailed global view (of the signal), and low scales correspond to a detailed view. Similarly, in terms of frequency, low frequencies (high scales) correspond to a global information of a signal (that usually spans the entire signal), whereas high frequencies (low scales) correspond to detailed information for a hidden pattern in the signal (that usually lasts a relatively short time).

Multifractal functions are used to model signals whose regularity may change abruptly from one point to the next (Jaffard 2004). In a physical context, this property holds only within a few magnitudes of change, the so called singularities in the signal (Vicsek 1992). The singularities are quantified by the Hölder exponent, obtained through the scale invariant property. The definition of statistical moments is used in the present work, where q is the order statistical moment. For more details on the subject see the papers by Arneodo et al. (1995) and McAteer et al. (2007). In our case, the continuous raw reflectance signal was submitted to a wavelet-based multifractal analysis to search for singularities. Thus, following the works of Posadas et al. (2003) and McAteer et al. (2007), wavelet transform modulus maxima and multifractal formalisms were applied to the data, aiming to detect such singularities and obtain the multifractal spectrum for each group, control and exposed plants.

Data pre-processing

In order to enhance the multifractal analysis, the raw reflectance signal was pre-processed. A raw signal is the primary reflectance signal measured and a pre-processed data is a signal that has been “transformed” by any of the available mathematical transformations—but

not yet submitted to multifractal analysis. Thus, a background correction was applied to the raw reflectance data to reduce both the variations caused by small atmospheric changes occurring while measuring all the plants within a day and the non-systematic measuring errors. The background correction was performed by the linear regression shown in Eq. 2. The slope and intercept of the regression were estimated by Eqs. 3 and 4.

$$S_j(\lambda_i) = A_j G_j(\lambda_i) + B_j \quad (2)$$

$$A_j = \frac{(G_{\max_j} - G_{\min_j})}{(G_{Total\max} - G_{Total\min})} \quad (3)$$

$$B_j = G_{\min_j} - A_j G_{Total\min} = G_{\max_j} - A_j G_{Total\max} \quad (4)$$

where $S_j(\lambda_i)$ and $G_j(\lambda_i)$ are the corrected and raw signals for the j th plant at the i th wavelength, respectively, G_{\max_j} and G_{\min_j} are the maximum and minimum raw measures of the j th plant, and $G_{Total\max}$ and $G_{Total\min}$ are the maximum and minimum raw measures of all the plants within a treatment, measured in a sampling date, A_j is the ratio of the response range of the j th plant to total population, B_j is the regression intercept.

The wavelet used for the multifractal analysis of the pre-processed data was the Morlet wavelet, included in the software Multifractal.f.pro, developed by the International Potato Center (CIP) from the original software by McAteer et al. (2007).

Statistical analysis

The response variables (raw spectra and multifractal parameters) were analyzed following the split plots in time design. In the main plot, plants were randomly assigned to each of the treatments to avoid biases in the allocation of plants. Reflectance measurements taken over time (or sub-plot) could not be randomized therefore a carry-over effect—i.e. observations close in time may be more related than observations far apart in time—could not be avoided. To minimize the bias introduced by this carry-over effect, repeated measurements were performed as explained by Wolfinger and Chang (1998). The analysis of variance generated by the General Linear Model (GLM) allows the determination of statistical differences between treatments, as a function of time, with a pre-established probability level (P value) of 5%. A significant difference indicates that, on the one hand, the variation due to treatment, at a particular time within the experiment, was greater than the variation among plants within each treatment. On the other hand, it indicates that the number of replicates was enough to reach a robust assessment of the differences between control and exposed plants. All the statistical analyses were performed with the SPSS 12.0 software package (SPSS Inc., Illinois, USA).

Results and discussion

The post enrichment NCM-ELISA laboratory test detected that 53 and 20% of the plants transplanted into the inoculated substrate—for the first and second experiments, respectively—were infected by the bacteria. However, only half of the infected plants presented visual symptoms in the first experiment and two-thirds in the second one. In other words, the latently infected plants—i.e. 50 and 33% of the plants with positive reactions in the NCM-ELISA test in the first and second experiments, respectively—could not be identified

Fig. 2 Scale invariance assessment for the reflectance data of healthy and infected plants. *Top*: Partition function of $h(q)$ as a function of wavelength scale at -2 and 2 values of q . *Bottom*: The partition function $D(h(q))$ as a function of wavelength scale with the same plot shades. The scale invariance were realized both Ctrl = control plants and Rs = symptomatic plants infected with *R. solanacearum*, respectively

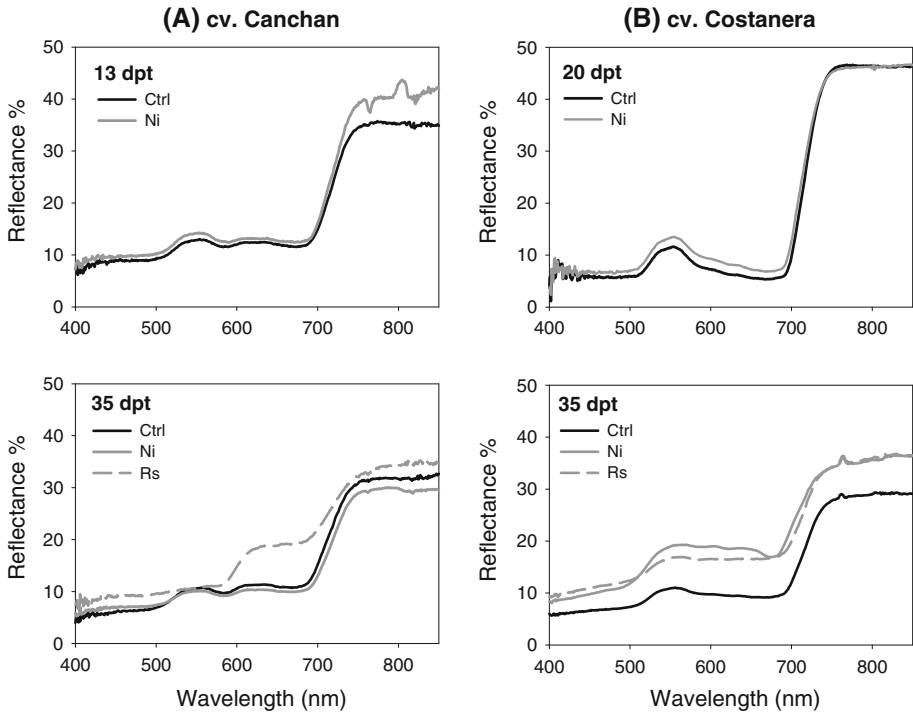
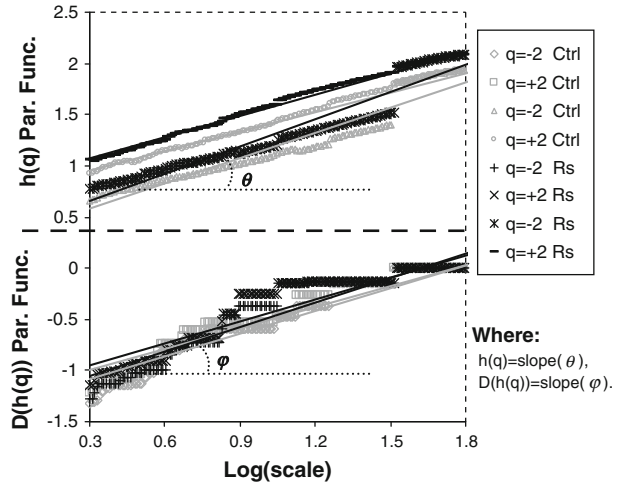


Fig. 3 Reflectance patterns of control and exposed potato plants (Ctrl = Control, Ni = Non-infected, Rs = symptomatic (infected) plants). Plants cv. Canchan (*left*) that developed the bacterial wilt disease (Rs) showed an increased reflectance in the blue and specially in the red bands of the electromagnetic spectra, keeping the green reflectance as constant but losing the typical spectra of vegetation. In contrast, Rs plants cv. Costanera (*right*) did show a moderate increase in blue, green and red light reflectance, but the spectrum kept the typical spectra of vegetation. (dpt = days post transplanting into soil inoculated with bacteria)

Fig. 4 Multifractal singularity spectra of plants with respective standard errors. First experiment with potato plants cv. Canchan (left column **a**) and second experiment with cv. Costanera (right, **b** column). (Ctrl = Control, Ni = Non-infected, Rs = symptomatic (infected) plants, dpt = days post transplanting into soil inoculated with bacteria)

as infected plants by visual assessment. This finding corroborates that relying exclusively on visual evaluation of bacterial wilt symptoms could be misleading.

Multifractal results

To apply the multifractal analysis to the reflectance signals obtained from control and exposed plants, the first step was to show that the pre-processed data presented multifractal attributes. The signal showed cusp-like and step-like singularities (Fig. 1). Then, the scale invariance property (linearity or physical-statistical laws along the scales) shown by both types of signals (Fig. 2) made the estimation of the multifractal singularity spectra and its parameters possible. The system showed linearity for the order moments q ranging from -2 to 2 , for both experiments.

Differences between control and exposed plants were not clearly shown by the raw reflectance spectra as the signals corresponding to infected asymptomatic and healthy control plants were similar (Fig. 3). However, the multifractal analysis enhanced the differences in multispectral reflectance, showing that infected plants, whether symptomatic or not, soon differed from control plants.

Figure 4 shows that the multifractal singularity spectra have more than one fractal dimension, which is a characteristic of multifractal systems. The resultant singularity spectra showed evident differences between the multifractal dimensions ($D_0 \equiv Dh(q = 0)$, $D_1 \equiv Dh(q = 1)$, and $D_2 \equiv Dh(q = 2)$) of healthy and infected plants. The values D_0 , D_1 and D_2 are known as the capacity, the entropy and the correlation dimensions, respectively. The capacity dimension provides global (or average) information about a system (Voss 1988). For example: the dimension $D_0 = 1, 2$, and 3 , represent the line, square and cube dimension, respectively, (often called Euclidean dimensions). For the $0 < D_0 < 1$ interval values, clusters of point values, discontinue lines and attractors are represented. For the $1 < D_0 < 2$ interval, curve lines and planes with holes are characterized. And for the $2 < D_0 < 3$ interval, curve planes or surfaces with or without holes and curve cubes are characterized and so on. Then, the capacity dimension D_0 (also called Fractal dimension) would be summarized as a parameter that describes the capacity of a signal to fill a Euclidean space. D_1 represents the entropy scale invariant value related to the information (or Shannon) entropy (Shannon and Weaver 1949). Entropy, in thermodynamics and information theory (Williams 1999), is a parameter that describes the energy not available for useful work in a thermodynamic process or as information. In our context, low entropy means that a large proportion of the system's information is obtainable. D_2 correlates long and short memory components, being the statistical component that expresses the associability or concurrence within signal values groups. Table 2 shows the differences in the capacity dimensions of the multifractal spectra taken from non-infected, latently infected and symptomatic plants from the 16th and 21st days after transplanting into the bacterial inoculated soil, for the first and second experiments, respectively. We focused on D_0 , since its computation is of simpler implementation and gave as good results as D_1 and D_2 . Figure 5 shows the results of our method based on the multifractal formalism. Each subject's dataset is characterized by three quantities: The first quantity (z -axis) is the degree of multifractality, which is the difference between the maximum and minimum values of local

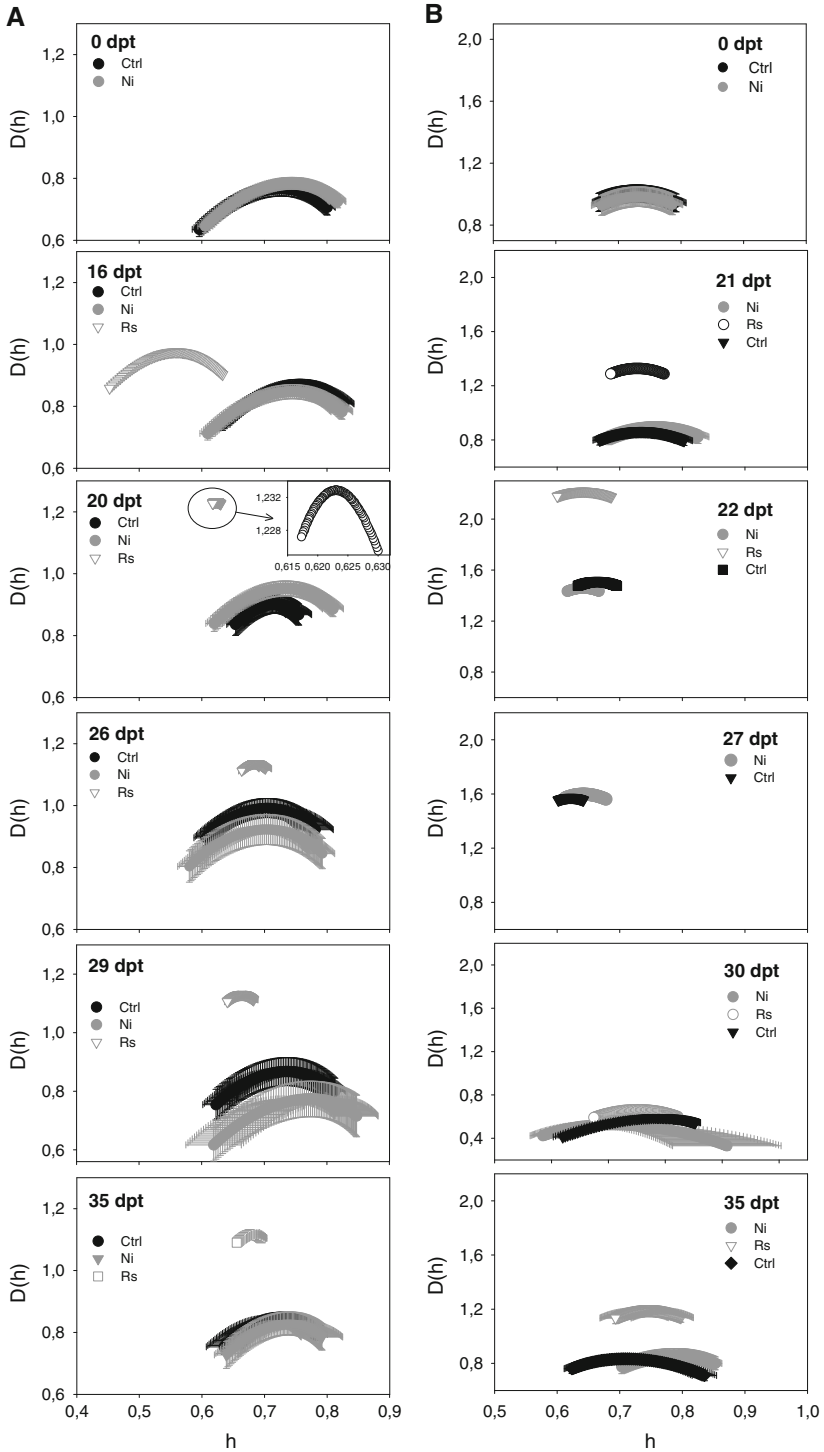


Table 2 Differences in the capacity or fractal dimension (D_0) between control and exposed (grown in *R. solanacearum* inoculated soil) plants in the first and second experiments

Days post transplanting in soil inoculated with bacteria	1st experiment $\Delta D_0 \pm MSE(D_{0Ctrl} - D_{0R_i})$		
	Non-infected	Actively infected	Latently infected
0	0.02 ± 0.004	0.02 ± 0.004	0.02 ± 0.004
10	0.11 ± 0.023	0.11 ± 0.023	0.11 ± 0.023
11	0.02 ± 0.002	0.02 ± 0.002	0.02 ± 0.002
13	0.01 ± 0.013	0.01 ± 0.013	0.01 ± 0.013
16	0.05 ± 0.005	0.17 ± 0.029	0.05 ± 0.005
17	0.01 ± 0.017	0.15 ± 0.023	0.01 ± 0.017
20	0.07 ± 0.012	0.18 ± 0.041	0.18 ± 0.041
23	0.07 ± 0.018	0.14 ± 0.031	0.07 ± 0.018
26	0.09 ± 0.013	0.26 ± 0.048	0.09 ± 0.013
29	0.04 ± 0.037	0.26 ± 0.379	0.04 ± 0.037
35	0.02 ± 0.018	0.27 ± 0.019	0.02 ± 0.018
Days post transplanting in soil inoculated with bacteria	2nd experiment $\Delta D_0 \pm MSE(D_{0Ctrl} - D_{0R_i})$		
	Non-infected	Actively infected	Latently infected
0	0.02 ± 0.008	0.02 ± 0.008	0.02 ± 0.008
21	0.03 ± 0.016	0.47 ± 0.032	0.39 ± 0.035
22	0.05 ± 0.006	0.71 ± 0.059	0.05 ± 0.006
27	0.02 ± 0.004	0.02 ± 0.004	0.02 ± 0.004
30	0.07 ± 0.005	0.08 ± 0.015	0.07 ± 0.005
35	0.03 ± 0.016	0.35 ± 0.035	0.03 ± 0.016

Hölder exponent h for each individual ($h_{\max} - h_{\min} = \Delta h$). If $\Delta h = 0$, the signal is monofractal (or of fractal behavior over all its physical laws), but if $\Delta h \neq 0$, it is multifractal (support more than one fractal dimension or shows more than one Dh value). The second quantity (y -axis) is the mass exponent value $\tau(q)$ characterizing the scaling of the q th moment. This τ is a multifractal parameter that provides insights about how much of the measure (or the signal) is concentrated or distributed with respect to each statistical q -th moment (Posadas et al. 2003). The third quantity (x -axis) is the standard deviation of the light reflectance signals. It is known that $\tau(q) = h(q) \cdot q - Dh(q)$, where q is the order moment (Halsey et al. 1986). So, for $q = 0$, the scaling exponent of the zero moment will be $\tau(q = 0) = -Dh(q = 0)$, then showing negative values for the x -axis in Fig. 5. More detailed information about the exponent τ is provided elsewhere e.g. Halsey et al. (1986), Vicsek (1992), Arneodo et al. (1995) and Posadas et al. (2003). Then, Fig. 5 shows the discrimination between control, non-infected, latently infected and symptomatic diseased plants.

The dates when the differences in the spectra were noticed matched the time when the visual inspection detected the first symptoms in infected plants in both experiments.

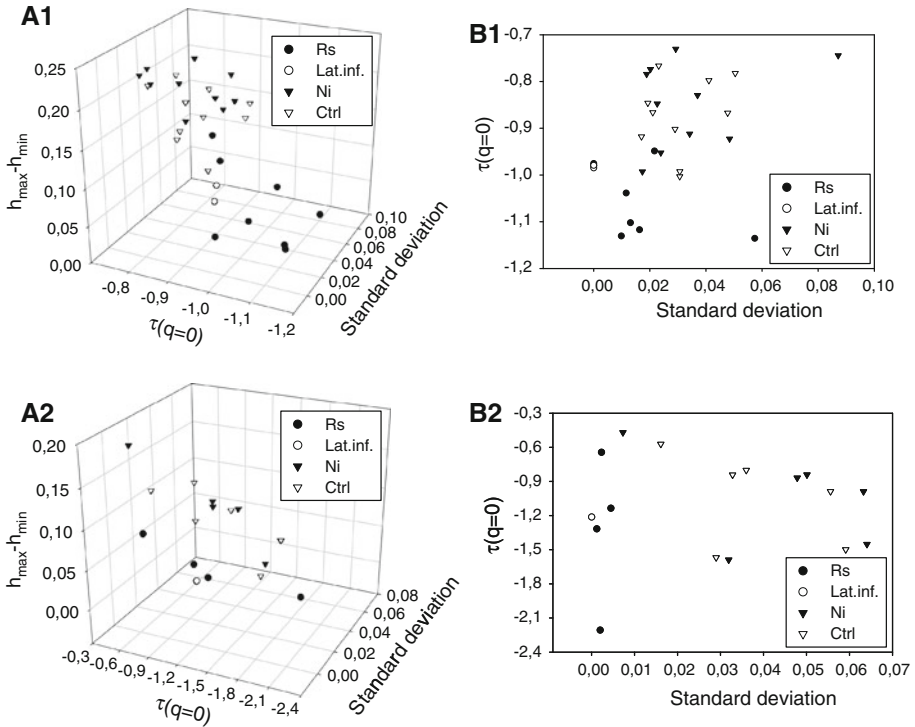


Fig. 5 Discrimination method based on the multifractal formalism, **a** Each subject’s dataset in the database is characterized by three quantities. The first quantity (*z*-axis) is the degree of multifractality, which is the difference between the maximum and minimum values of local Hurst exponent *h* for each individual ($h_{\max} - h_{\min} = \Delta h$). If $\Delta h = 0$, the signal is monofractal, but if $\Delta h \neq 0$, it is multifractal. The second quantity (*y*-axis) is the mass exponent value $\tau(q)$ characterizing the scaling of the *q*-th moment. The third quantity (*x*-axis) is the standard deviation of the light reflectance signals. **b** Discrimination method based on multifractal formalism in the *x*–*y* axis. The *y*-axis is the exponent value $\tau(q = 0)$, and the *x*-axis is the standard deviation of the time series of light reflectance signals. (Ctrl = Control, Ni = Non-infected, Rs = symptomatic (infected), Lat.inf. = Latently infected plants)

The criteria for defining a plant grown in inoculated substrate as non-infected, latently infected, or symptomatic was based on its multifractal spectra response. Thus, a plant was identified as symptomatic when the intermittent response of the multifractal spectra of any particular plant reached a steady state of significant difference (P -value < 0.05) with respect to control plants. In contrast, when the intermittent response of the multifractal spectra of any particular plant grown in inoculated substrate eventually reached a steady state that did not differ significantly from the spectra from control plants, it was considered as a latently infected plant. On the other hand, when the multifractal spectra of a plant grown in inoculated substrate did not ever differ significantly from the spectra from control plants it was deemed as uninfected. For the first experiment, 100% detection of the total infected plants (8 out of 8) was achieved by the multifractal spectra response although three of them were regarded as latently infected as no symptoms were noticed. Confirmation of disease in those latently infected plants was obtained through the ELISA test. In the second experiment also, with cv. Costanera, the multifractal analysis correctly discriminated both the symptomatic and latently infected plants (Table 2) but 5 days earlier

than in the first experiment with cv. Canchán. Costanera is described as a *R. solanacearum* resistant cultivar (CIP 2008). The capability of remotely sensing light reflectance and concomitant multifractal analysis of the signal to detect damage caused by bacteria is dependent on changes in reflectance brought about by blockage of vascular tissue in infected plants (Grimault et al. 1994; Hernández et al. 2005). Also, the discrimination of healthy, diseased and latently-infected plants might be related to the tyloses, structures whose formation is associated with response to stress caused either by pathogens or other factor (Agrios 2005). Grimault et al. (1994) observed that tyloses occurred in inoculated tomato cultivars resistant to *R. solanacearum*, whereas in susceptible cultivars such structures were not formed.

Discrete reflectance bands and vegetation indexes

A distinct reflectance pattern from infected plants was evident, mainly within the visible region of the electromagnetic spectrum, 1 day after both the visual evaluation and the multifractal analysis of multispectral data were able to detect first initial symptoms of disease, i.e. 16 and 21 days post transplanting into *R. solanacearum*-inoculated substrate for the first and second experiment, respectively (P -value < 0.05). The response was consistent in all exposed plants. The most suitable bands for detecting the bacterial wilt infection were the blue (P -value < 0.01) and the red regions (P -value < 0.01). Unlike the sustained discrimination feasible with multifractal spectra, where the differences in the parameters of the multifractal spectrum were maintained for a longer time, particularly for susceptible *R. solanacearum* varieties, the detection window using discrete bands seems to be very short and variable and might require frequent assessments to avoid missing the reflectance difference produced by infected plants. In contrast, both the green and the NIR regions of the electromagnetic spectrum were not reliable indicators of *R. solanacearum* stress. Particularly the NIR showed no change, being of no use for revealing differences between the treatments (Fig. 6).

Spectral vegetation indexes tested showed an inconsistent and unreliable response (Fig. 7), likely due to their dependency on a few optimal wavebands and discarding the majority of the spectrum (Blackburn and Ferwerda 2008).

Our results indicate that blue light reflectance increased in infected plants, which means a reduction of blue light absorbance. In contrast, red light reflectance did not increase as markedly as blue light, and even in some stressed plants it did not vary. This could be related to the action of accessory light-harvesters and photo-protector pigments that were unaffected by stress. This, together with the chloroplasts movements in the cells to avoid strong light/elevated temperature situations (Wada et al. 2003), could explain why blue reflectance always increased under a stress situation. In fact, in pathogen resistant plant varieties, the accessory pigments and their sub-products (i.e. phenolic compounds) have additional defense properties against pathogens, so plants appear yellow and/or red at the site of infection or attack due to a higher synthesis of those sub-products as a reaction, as seen in the *R. solanacearum* resistant potato cultivar Costanera.

Conclusions

Reflectance patterns in the 350–850 nm region of the electromagnetic spectrum, processed through multifractal analysis, was able to detect bacterial wilt infected plants at the same time as the expert trained eye in 100% of the observations. Furthermore, the multispectral

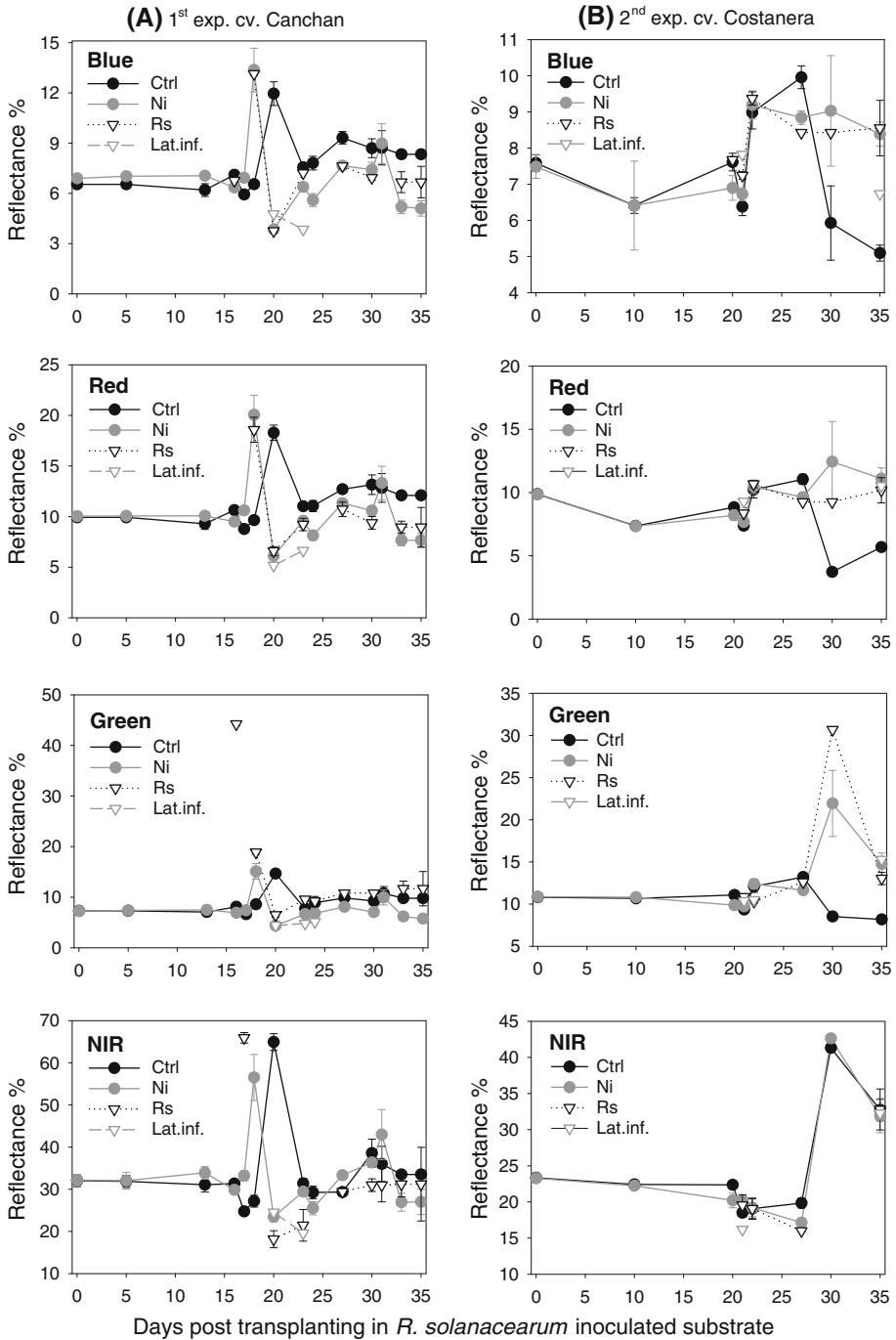
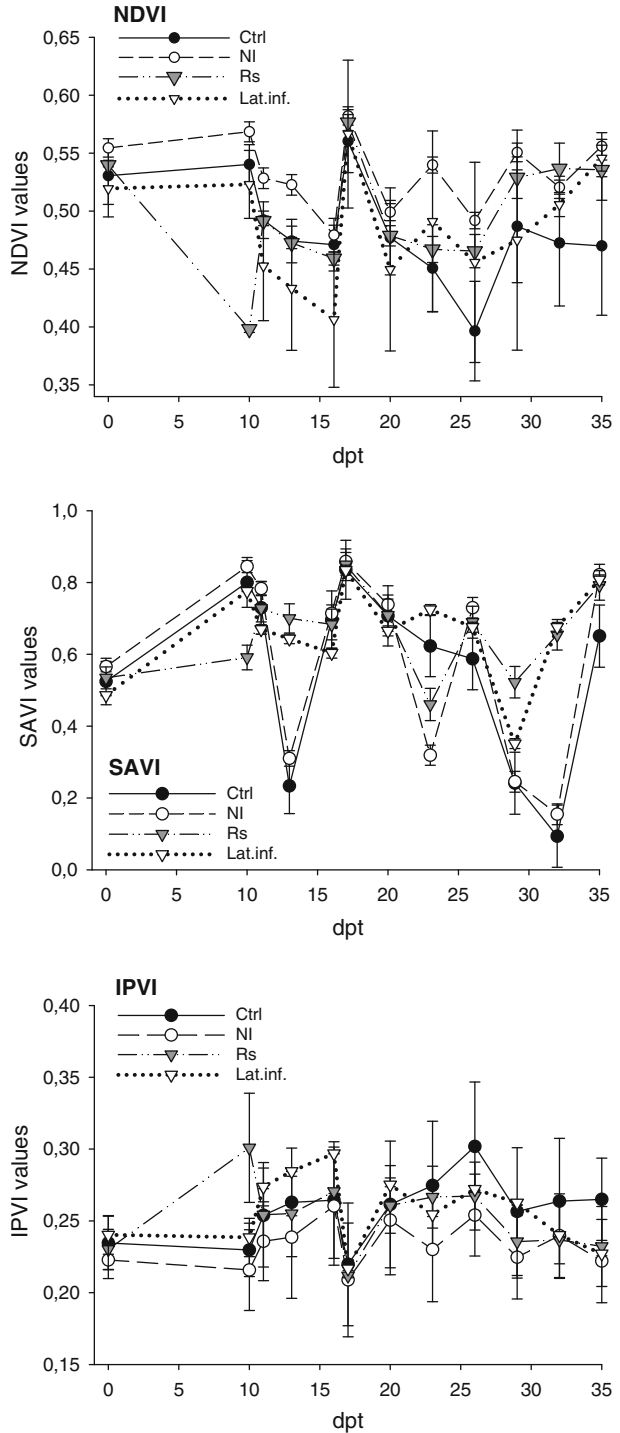


Fig. 6 Discrete bands of plants' reflectance mimicking those of satellite Landsat TM, blue (450–520 nm), green (520–600 nm), red (630–690 nm), NIR (760–900 nm). First experiment (a, left) and second experiment (b, right). (Ctrl = Control, Ni = Non-infected, Rs = symptomatic (infected), Lat.inf. = Latently infected plants)

Fig. 7 Behavior of three of the spectral vegetation indices calculated from spectroradiometric data in the first experiment. (Ctrl = Control, NI = Non-infected, Rs = symptomatic (infected), Lat.inf. = Latently infected plants, dpt = days post transplanting into soil inoculated with bacteria)



and multifractal analyses were able to detect asymptomatic plants (not detected at all by the trained eye), achieving a success rate that was on average about 82% of the diagnostic achieved by the CIP post enrichment NCM-ELISA laboratory assessment. Although several multifractal parameters can be used in the detection, the capacity or fractal dimension, which can be easily estimated, was as robust a discriminator as the entropy or correlation dimensions. It is also important to point out that the direct reflectance in the blue and red regions of the electromagnetic spectrum were also sensitive to the presence of *R. solanacearum* symptoms, albeit for a short period of time.

The fact that it is possible to illustrate a distinct reflectance pattern for stressed plants at several wavelengths within the multispectral section of the electromagnetic spectrum is a useful finding for researchers with access to a spectroradiometer or remotely sensed imageries over a range of wavelengths (e.g. SPOT, AVIRIS). Also, discrete ranges of the spectrum would be useful and could be used by discontinuous sensors, such as ground-based or air- and space-borne multispectral cameras.

The proposed reflectance-based method could be a practical and cost-effective tool with a high utilization potential for precision agriculture in a plant health monitoring program, as it could help farmers to have both a more focalized and timely response to intra-field and intra-crop variations such as the outbreak of disease, which tends to be patchy. However, further research must be carried out to improve the proposed remote sensing approach.

Acknowledgments Support for this work was provided by the International Foundation for Science (IFS Grant 4068/I), the Production Systems and the Environment Division of the International Potato Center (CIP) and the CIP-ALTAGRO project. The authors thank Eng. Liliam Gutarra from the Integrated Crop Management Division at CIP for her support on laboratory assessments, and to R.T.J. McAteer and collaborators for kindly sharing their wavelet-multifractal algorithm. P. Chávez gives special thanks to Arnauld A. Thiry for his permanent and unconditional support, and Drs. Salomón Helfgott and Vicente Rázuri from La Molina Agricultural University for their good advices.

References

- Agrios, G. N. (2005). *Plant pathology* (5th ed.). San Diego, CA: Academic Press.
- Allen, C., Kelman, A., & French, E. R. (2001). Brown rot of potatoes. In W. R. Stevenson, R. Loria, G. D. Franc, & D. P. Weingartner (Eds.), *Compendium of potato diseases* (pp. 11–13). St. Paul, MN: The American Phytopathological Society.
- Arneodo, A., Bacry, E., Graves, P. V., & Muzzy, J. F. (1995). Characterizing long-range correlations in DNA sequences from wavelet analysis. *Physical Review Letters*, *74*(16), 3293–3296.
- Bacry, E., Muzy, J. F., & Arnéodo, A. (2003). Singularity spectrum of fractal signals from wavelet analysis: Exact results. *Journal of Statistical Physics*, *70*(3–4), 635–674.
- Blackburn, G. A., & Ferwerda, J. G. (2008). Retrieval of chlorophyll concentration from leaf reflectance spectra using wavelet analysis. *Remote Sensing of Environment*, *112*(4), 1614–1632.
- Broge, N. H., & Leblanc, E. (2000). Comparing prediction power and stability of broadband and hyperspectral vegetation indices for estimation of green leaf area index and canopy chlorophyll density. *Remote Sensing of Environment*, *76*(2), 156–172.
- Buchanan-Wollaston, V. (1997). The molecular biology of leaf senescence. *Journal of Experimental Botany*, *48*(2), 181–199.
- Byalovskii, Y. Y., Bulatetskii, S. V., & Suchkova, Z. V. (2005). Heart rate variability and fractal neurodynamics during local magnetic vibroacoustic treatment. *Human Physiology*, *31*(4), 413–420. Translated from *Fiziologiya Cheloveka*, *431*(414), 450–460.
- CABI. (2003). *Crop protection compendium: Global module* (5th ed.). Wallingford, UK: CAB International.
- Chávez, P., Yarlequé, C., Piro, O., Posadas, A., Mares, V., Loayza, H., et al. (2010). Applying multifractal analysis to remotely sensed data for assessing PVYV infection in potato (*Solanum tuberosum* L.) crops. *Remote Sensing Journal*, *2*(5), 1197–1216.

- Chávez, P., Zorogastúa, P., Chuquillanqui, C., Salazar, L. F., Mares, V., & Quiroz, R. (2009). Assessing Potato Yellow Vein Virus (PYVV) infection using remotely sensed data. *International Journal of Pest Management*, 55, 251–256.
- Chhabra, A. B., Jensen, R. V., & Sreenivasan, K. R. (1989a). Extraction of underlying multiplicative processes from multifractals via the thermodynamic formalism. *Physical Review A*, 40(8), 4593–4611.
- Chhabra, A. B., Meneveau, C., Jensen, R. V., & Sreenivasan, K. R. (1989b). Direct determination of the $f(a)$ singularity spectrum and its application to fully developed turbulence. *Physical Review A*, 40(9), 5284–5294.
- Chiwaki, K., Nagamori, S., & Inoue, Y. (2005). Predicting bacterial wilt disease of tomato plants using remotely sensed thermal imagery. *Journal of Agricultural Meteorology*, 61, 153–164.
- CIP-International Potato Center. (2008). *Review of nematology activities at CIP* (p. 16). <https://research.cip.cgiar.org/confluence/download/attachments/16679035/Report+on+Nematology+at+CIP+1999+Author+Maria+Scurrah+-1.pdf?version=1>. Accessed 1 March 2010.
- Cook, D., Barlow, E., & Sequeira, L. (1989). Genetic diversity of *Pseudomonas solanacearum*: Detection of restriction fragment length polymorphism with DNA probes that specify virulence and the hypersensitive response. *Molecular Plant-Microbe Interactions*, 2, 113–121.
- Cook, D., & Sequeira, L. (1994). Strain differentiation of *Pseudomonas solanacearum* by molecular genetic methods. In A. C. Hayward & G. L. Hatman (Eds.), *Bacterial Wilt: The disease and its causative agent, Pseudomonas solanacearum* (pp. 77–93). Wallingford, UK: CAB International.
- Crippen, R. E. (1990). Calculating the vegetation index faster. *Remote Sensing of Environment*, 34(1), 71–73.
- Daughtry, C. S. T., Walthall, C. L., Kim, M. S., Brown de Colstoun, E., & McMurtrey III, J. E. (2000). Estimating corn leaf chlorophyll concentration from leaf and canopy reflectance. *Remote Sensing of Environment*, 74(2), 229–239.
- Elphinstone, J. G. (1996). Survival and possibilities for extinction of *Pseudomonas solanacearum* (Smith) in cool climates. *Potato Research*, 39, 403–410.
- Fock, I., Collonnier, C., Luisetti, J., Purwito, A., Souvannavong, V., Vedel, F., et al. (2001). Use of *Solanum stenotomum* for introduction of resistance to bacterial wilt in somatic hybrids of potato. *Plant Physiology and Biochemistry*, 39, 899–908.
- French, E. R., Gutarra, L., Aley, P., & Elphinstone, J. (1995). Culture media for *Pseudomonas solanacearum*: Isolation, identification and maintenance. *Fitopatologia*, 30, 126–130.
- Gamon, J. A., Peñuelas, J., & Field, C. B. (1992). A narrow-waveband spectral index that tracks diurnal changes in photosynthetic efficiency. *Remote Sensing of Environment*, 41(1), 35–44.
- Grimault, V., Gelie, B., Lemattre, M., Prior, P., & Schmit, J. (1994). Comparative histology of resistant and susceptible tomato cultivars infected by *Pseudomonas solanacearum*. *Physiological and Molecular Plant Pathology*, 44, 105–123.
- Habashy, W. H. S., Fawzi, F. G., El-Huseiny, T. M., & Neweigy, N. A. (1993). Bacterial wilt of potatoes. II. Sensitivity of the pathogen to antibiotics and pathogenesis by streptomycin-resistant mutants. *Egyptian Journal of Agricultural Research*, 71, 401–412.
- Haboudane, D., Miller, J. R., Tremblay, N., Zarco-Tejada, P. J., & Dextraze, L. (2002). Integrated narrowband vegetation indices for prediction of crop chlorophyll content for application to precision agriculture. *Remote Sensing of Environment*, 81(2–3), 416–426.
- Haboudane, D., Miller, J. R., Pattey, E., Zarco-Tejada, P. J., & Strachan, I. B. (2004). Hyperspectral vegetation indices and novel algorithms for predicting green LAI of crop canopies: Modeling and validation in the context of precision agriculture. *Remote Sensing of Environment*, 90(3), 337–352.
- Halsey, T. C., Jensen, M. H., Kanadoff, L. P., Procaccia, I., & Shraiman, B. (1986). Fractal measures and their singularities: The characterization of strange sets. *Physical Review A*, 33(2), 1141–1151.
- Hartman, G. L., & Elphinstone, J. G. (1994). Advances in the control of *Pseudomonas solanacearum* Race 1 in major food crops. In A. C. Hayward & G. L. Hatman (Eds.), *Bacterial Wilt: The disease and its causative agent, Pseudomonas solanacearum* (pp. 157–177). Wallingford, UK: CAB International.
- Hayward, A. C. (1964). Characteristics of *Pseudomonas solanacearum*. *Journal of Applied Bacteriology*, 27, 265–277.
- Hayward, A. C. (1991). Biology and epidemiology of bacterial wilt caused by *Pseudomonas solanacearum*. *Annual review of Phytopathology*, 29, 65–87.
- Hernández, Y., Marino, N., Trujillo, G., & Urbina de Navarro, C. (2005). Invasión de *Ralstonia solanacearum* en tejidos de tallos de tomate (*Lycopersicon esculentum* Mill). *Revista de la Facultad de Agronomía*, 22(2), 185–194.
- Huete, A. R. (1988). A soil-adjusted vegetation index (SAVI). *Remote Sensing of Environment*, 25(3), 295–309.

- Inoue, Y. (1990). Remote detection of physiological depression in crop plants with infrared thermal imagery. *Japanese Journal of Crop Science*, 59, 762–768.
- Ivanov, P. C., Nunes Amaral, L. A., Goldberger, A. L., Havlin, S., Rosenblum, M. G., Struzik, Z. R., et al. (1999). Multifractality in human heartbeat dynamics. *Nature*, 399, 461–465.
- Jaffard, S. (2004). Wavelet techniques in multifractal analysis, fractal geometry and applications. In: AMS (Ed.), *Proceedings of symposia in pure mathematics* (pp. 91–152). Providence, RI.
- Janse, J. D. (1996). Potato brown rot in Western Europe—History, present occurrence and some remarks on possible origin, epidemiology and control strategies. *Bulletin OEPP*, 26, 679–695.
- Latka, M., Glaubic-Latka, M., Latka, D., & West, B. (2002). The loss of multifractality in migraines. http://arxiv.org/PS_cache/physics/pdf/0204/0204010v1.pdf.
- López, M. M., & Biosca, E. G. (2004). Potato bacterial wilt management: New prospects for an old problem. In C. Allen, P. Prior, & A. C. Hayward (Eds.), *Bacterial wilt disease and the Ralstonia species complex* (pp. 205–224). St. Paul, MN: APS Press.
- McAteer, R. T. J., Young, C. A., Ireland, J., & Gallagher, P. T. (2007). The bursty nature of solar flare X-ray emission. *The Astrophysical Journal*, 662, 691–700.
- Mendoza, H. A. (1994). Development of potatoes with multiple resistance to biotic and abiotic stresses: The International Potato Center Approach. In G. W. Zehnder, M. L. Powelson, & R. Jansson (Eds.), *Advances in potato pest biology and management* (pp. 627–642). St. Paul, MN: American Phytopathological Society.
- Murakoshi, S., & Takahashi, M. (1984). Trials of some control of tomato wilt caused by *Pseudomonas solanacearum*. *Bulletin of the Kanagawa Horticultural Experiment Station*, 31, 50–56.
- Muzy, J. F., Bacry, E., & Arneodo, A. (1991). Wavelets and multifractal formalism for singular signals: Application to turbulence data. *Physical Review Letters*, 67, 3515–3518.
- Parrott, N., & Kalibwani, F. (2004). Organic agriculture in the continents, Africa. In H. Willer & M. Yussefi (Eds.), *The world of organic agriculture statistics and emerging trends* (pp. 55–68). Bonn, Germany: International Federation of Organic Agriculture Movements.
- Polikar, R. (1996). *The wavelet tutorial*. <http://users.rowan.edu/~polikar/WAVELETS/WTpart1.html>. Accessed 1 March 2010.
- Posadas, A. N. D., Giménez, D., Quiroz, R. A., & Protz, R. (2003). Multifractal characterization of soil pore systems. *Soil Science Society of America Journal*, 67, 1361–1369.
- Posadas, A. N. D., Quiroz, R., Zorogastúa, P., & León-Velarde, C. (2005). Multifractal characterization of the spatial distribution of Ulexite in a Bolivian salt flat. *International Journal of Remote Sensing*, 26, 615–627.
- Prior, P., & Fegan, M. (2005). Recent developments in the phylogeny and classification of *Ralstonia solanacearum*. *Acta Horticulturae (ISHS)*, 695, 127–136.
- Priou, S., Gutarra, L., & Aley, P. (1999). Highly sensitive detection of *Ralstonia solanacearum* in latently infected potato tubers by post-enrichment enzyme-linked immunosorbent assay on nitrocellulose membrane. *EPPO/OEPP Bulletin*, 29, 117–125.
- Rondeaux, G., Steven, M., & Baret, F. (1996). Optimization of soil-adjusted vegetation indices. *Remote Sensing of Environment*, 55(2), 95–107.
- Rouse, J. W., Haas, R. H., Schell, J. A., Deering, D. W., & Harlan, J. C. (1974). *Monitoring the vernal advancement of retrogradation (green wave effect) of natural vegetation*. Final Report, Type III, NASA/GSFC, Greenbelt, MD, p. 371.
- Schaad, N. W. (1988). *Laboratory guide for identification of plant pathogenic bacteria* (164 pp.). St. Paul, MN: American Phytopathological Society.
- Schertzer, D., & Lovejoy, S. (1989). Nonlinear variability in geophysics: Multifractal analysis and simulation. In L. Pietronero (Ed.), *Fractals: Physical origin and consequences* (pp. 49–79). New York: Plenum.
- Schertzer, D., & Lovejoy, S. (2004). Uncertainty and predictability in geophysics: Chaos and multifractal insights. In R. S. J. Sparks & C. J. Hawkesworth (Eds.), *State of the planet, frontiers and challenges in geophysics* (pp. 317–334). Washington DC: American Geophysical Union.
- Shannon, C. E., & Weaver, W. (1949). *The mathematical theory of communication*. Urbana, IL: University of Illinois Press.
- Swanson, J. K., Yao, J., Tans-Kersten, J., & Allen, C. (2005). Behavior of *Ralstonia solanacearum* race 3 biovar 2 during latent and active infection of geranium. *Phytopathology*, 95, 136–143.
- Sylvander, B., & Le Floc'h-Wadel, A. (2000). Consumer demand and production of organics in the EU. *AgBioForum*, 3, 97–106.
- University of Arizona. (2005). *Remote sensing of vegetation*. <http://rangeview.arizona.edu/Tutorials/intro.asp>. Accessed 9 May 2011.

- van Elsas, J. D., Kastelein, P., de Vries, P. M., & van Overbeek, L. S. (2001). Effects of ecological factors on the survival and physiology of *Ralstonia solanacearum* bv. 2 in irrigation water. *Canadian Journal of Microbiology*, *47*, 842–854.
- van Elsas, J. D., Kastelein, P., van Bekkum, P., van der Wolf, J. M., de Vries, P. M., & van Overbeek, L. S. (2000). Survival of *Ralstonia solanacearum* biovar 2, the causative agent of potato brown rot, in field and microcosm soils in temperate climates. *Phytopathology*, *90*, 1358–1366.
- Vicsek, T. (1992). *Fractal growth phenomena* (2nd ed.). Singapore: World Scientific Publishing Co.
- Voss, R. F. (1988). Fractals in nature: From characterization to simulation. In H.-O. Peitgen & D. Saupe (Eds.), *The science of fractal images* (pp. 21–70). New York: Springer.
- Wada, M., Kagawa, T., & Sato, Y. (2003). Chloroplast movement. *Annual Review of Plant Biology*, *54*, 455–468.
- Weingartner, D. P., & Shumaker, J. R. (1988). In row injection of metham sodium and other soil fumigants for control of nematodes and soil borne potato diseases in Florida. 72nd Annual Meeting of the Potato Association of America, Fort Collins, Colorado, USA. *American Potato Journal*, *65*, 504.
- Williams, G. C. (1999). Pleiotropy, natural selection and the evolution of aging. *Evolution*, *11*, 398–411.
- Williamson, L., Nakaho, K., Hudelson, B., & Allen, C. (2002). *Ralstonia solanacearum* race 3, biovar 2 strains isolated from geranium are pathogenic on potato. *Plant Disease*, *86*, 987–991.
- Wolfinger, R. D., & Chang, M. (1998). *Comparing the SAS GLM and MIXED procedures for repeated measures*. Cary, NC: SUGI Proceedings.
- Yu, Z.-G., Anh, V., & Lau, K.-S. (2001). Multifractal characterisation of length sequences of coding and noncoding segments in a complete genome. *Physica A: Statistical Mechanics and its Applications*, *301*, 351–361.